Fault Ride Through Strategy of DFIG Using Rotor Voltage Direct Compensation Control Under Voltage Phase Angle Jump

Xinshou Tian, Weisheng Wang, Xiang Li, Yongning Chi, Yan Li, and Haiyan Tang

Abstract—**Wind power experiences fast development during recent years, and large-scale wind power connected to power grid will bring a lot of new challenges. Some new operation characteristics in power grid with doubly-fed induction generator (DFIG) may present, for example the voltage phase angle jump. Voltage phase angle jump can potential make negative impacts on the fault ride through (FRT) performances of DFIG. Firstly, this paper investigates the physical mechanism and the operation characteristics of DFIG with voltage phase angle jump. It is noted that the current control strategies designed for the voltage amplitude change are not suitable for voltage phase angle jump. Then, based on the voltage phase angle deviation, this paper develops a FRT control strategy of DIFG using rotor voltage direct compensation control under voltage phase angle jump. It can optimize operation characteristics, develop FRT capability of DFIG. Finally, the simulation results of a 250MW wind farm is presented to validate the availability and effectiveness of proposed FRT control strategy.**

Index Terms—**DFIG, Voltage phase angle jump, Rotor voltage direct compensation control, FRT strategy.**

I. Introduction

The commercial development of wind turbines have increased over the past decades, and the installed capacity of wind power has arrived 128.3GW by the end of 2015 in China [1]. Due to the smaller converter rating and the lower cost, DFIG are widely equipped in wind farms [2]. However, most wind farms usually locate at the end of power grid, where a little system disturbance should cause a complex dynamic process of DFIG based wind turbines [3].

Because the power electronics devices is usually used in non-synchronous generator, the voltage phase angle of DFIG isn't related to the rotor position like synchronous generator does, and the voltage phase angle will jump if there is a serious grid fault [4]. At the same time, the using of phase-locked loop (PLL) increases the difficulty of designing FRT strategy and analyzing transient characteristics [5]. It is very important to maintain the security and reliability of power grid with large-scale wind turbines integration [6-7].

Nowadays, the FRT operation of wind farm is a basic and essential requirement for enhancing the transient stability of power grid [8]. Several papers have investigated the transient response characteristics and developed the FRT strategies of DFIG under voltage amplitude dip. In [9-11], it is discussed how to use the crowbar protection device of DFIG. Then, in [12, 13], the improved rotor excitation control strategies are proposed for FRT operation. Then, in [14], a coordinated control strategy among the series-dynamic-resistor, dc-link chopper and crowbar is presented. Some experts also focus on the impacts on transient stability of power grid [15-16].

The mechanism on voltage phase angle jump and its influence factors of DFIG are given on the basis of mathematical deduction [4]. The jump value is analyzed using grid fault analysis model [17]. A stochastic prediction of sags analytical method is used for better understanding the phase angle jump phenomenon [18]. However, the description of voltage phase angle jump physical mechanism is insufficient. Secondly, the influence of generator parameters and voltage phase angle jump on the transient process is analyzed [19-20]. Fault current characteristics of DFIG under voltage phase angle jump are analyzed [21-22], and the rotor voltage dynamic characteristics of DFIG with phase angle jump during the LVRT period are studied [23]. But the researches on the impact of voltage phase angle jump on PLL, FRT control characteristics of DFIG and their coupling are lack. Thirdly, in order to solve the phase-locked accuracy problem, some voltage synchronous signal detection methods are given, for example resonant compensator [24], sinusoidal amplitude integrator methods [25] and model reference adaptive algorithms [26] etc. In order to measure voltage dip and calculate phase angle jump value, six methods are proposed and compared [27]. The impacts of PLL on DFIG based on electromechanical time-scale response are given [28]. In addition, a phase angle compensation principle based FRT control strategy is given [29]. But the currently FRT control strategy of DFIG for voltage phase angle jump is lack of theoretical basis. The voltage phase angle jump broken the active power and reactive power decoupling control of DFIG,

Manuscript received November 11, 2016; revised ****, 2017; accepted ****, 2017. Date of publication ****, 2017; date of current version ****, 2017. This work was supported by Chinese National Natural Science Funds (51577174).

X.S. Tian (corresponding author, e-mail: tianxinshou@epri.sgcc.com.cn), W.S. Wang, Y.N. Chi, Y. Li and H.Y. Tang are with State Key Laboratory of Operation and Control of Renewable Energy & Storage Systems (China Electric Power Research Institute), Beijing 100192, China.

X. Li is with State Grid Beijing Changping Electric Power Supply Company, Beijing 100031, China.

DOI:

weaken the FRT capability, and may cause FRT failure of DFIG, so the traditional FRT strategy of DFIG will face some new technical challenges.

This paper reveals the operation characteristics of DFIG under voltage phase angle jump, and proposes a novel FRT strategy of DFIG for the safe operation of the power grid with large-scale DFIG integration. The paper will be organized as follows. Section II reveals the terminal voltage phase angle jump physical mechanism. In Section III, the operation characteristics of DFIG under voltage phase angle jump are discussed. Then, Section IV proposes a FRT strategy of DFIG using rotor voltage direct compensation control. In Section V, the simulation results are given to validate the effectiveness. Finally, Section VI makes the conclusions.

II. TERMINAL VOLTAGE PHASE JUMP CHARACTERISTIC OF DFIG CONNECTED TO POWER GRID

If there is a serious grid fault, the terminal voltage amplitude of DFIG drops, and the terminal voltage phase angle of DFIG would jump due to no inertia of the power electronics. Thus, the voltage phase angle characteristic of DFIG is different from the traditional synchronous generator. This section is aimed to reveal the voltage phase angle jump physical mechanism of DFIG, and then evaluate the voltage phase angle jump value.

A. Voltage phase angle jump physical mechanism of DFIG

The internal voltage of synchronous generator is produced on the basis of the electromagnetic response theory and the multi-phase winding modulation theory. The internal voltage of synchronous generator meets the rotor motion equation (1). The dynamic characteristics of internal voltage is dependent on the operation status of mechanical energy storage element driven by the torque imbalance between the mechanical torque and the electromagnetic torque. The dynamic characteristics of the internal voltage in synchronous generator are restricted by the inertia and damping of synchronous generator, which are electromechanical time-scale dynamics. Therefore, the change of internal voltage phase angle is slower [30].

$$J\frac{d^2\theta}{dt} = T_m - T_e \tag{1}$$

Where, J is the rotate inertia, θ is the phase angle, t is the time, T_m is the mechanical torque, T_e is the electromagnetic torque of synchronous generator.

However, due to the decoupling between the electrical parts and the mechanical parts of DFIG, the dynamic physical process of DFIG is completely different from the synchronous generator. The diagram of DFIG is shown in Fig. 1.

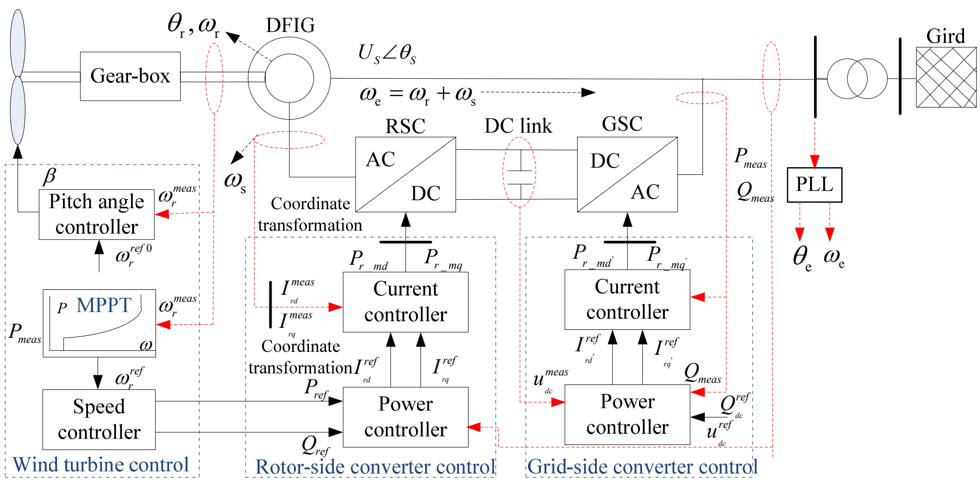

Fig. 1 Diagram of DFIG with the vector control method.

As shown in Fig. 1, the power electronic converters are usually adopted in DFIG. The internal voltage of DFIG is produced based on the multi-time-scale control strategy and the pulse width modulation theory. The physical mechanism on the inertia response of the power electronic equipment is the same with the internal voltage of wind turbines driven by the active power imbalance. Therefore, the dynamic characteristics of the internal voltage depend on the operation status of multi-scale energy storage element driven by the active power imbalance and the control characteristics of the energy storage element. The voltage phase angle of DFIG can be expressed as (2).

$$\theta_s = \omega_e t \tag{2}$$

Where, θ_s is the synchronous phase angle, ω_e is the synchronous angular speed.

The synchronous angular speed is represented by (3).

$$\omega_e = \omega_r + \omega_s \tag{3}$$

Where, ω_s is the slip angular speed.

The rotor rotational angular speed ω_r of DFIG meets the rotor motion equation (4), which is one-order differential equation of rotor speed. Therefore, the change of rotor rotational angular speed is slower.

$$M_D\frac{d\omega_r}{dt} = P_T - P_E \tag{4}$$

Where, M_D is the rotor inertia time constant, P_m is the mechanical power of DFIG, P_E is the electromagnetic power of DFIG.

However, the slip angular speed ω_s is given by (3), which is the rotation speed of rotor excitation magnetic field and implemented by the control of rotor-side converter (RSC). So the dynamic characteristics of slip angular speed are associated with the control strategies and control parameters of RSC. According to (2) and (3). The synchronous angular speed shows an electrical feature, and the internal voltage phase angle change of DFIG is faster. The transient process of voltage phase angle is decided by slip angular speed under grid fault. Where, the voltage phase angle change is an electromagnetic transient process. The voltage phase angle jumps if there is a serious grid fault, which influence the stability of power grid.

The voltage phase angle jump of DFIG is mainly affected by control strategies of RSC, but the impacts of grid-side converter (GSC) is relatively smaller, which can be thereby neglected. The reasons are as follows. 1) The capacity of DFIG is bigger than that of converter, so the impacts of control strategy of GSC on the stability of power grid is smaller. 2) The optimized control strategy of RSC is implemented to improve the FRT of DFIG. Therefore, it is smaller impact of control strategy of GSC to transient characteristics of DFIG. 3) The features on control strategy of GSC are to keep the DC capacitor voltage stability and make no reactive power exchange between power grid and GSC. The safety of DC capacitor can be guaranteed by chopper protection circuit, and a slight fluctuation is allowed in DC capacitor.

B. Assessment of voltage phase angle jump value of DFIG

There are already many studies on the model and controller of DFIG. It is shown that the fifth-order mathematical model of DFIG represents the completely dynamics characteristics, and the effectiveness of the model has been also verified. At the same time, the transient process of DFIG can also be analyzed based on the model. The stator and rotor voltage vector model of DFIG can be expressed by (5) and (6) respectively in the *dq* rotating reference frame [3].

$$\begin{cases} u_{sd} = \dfrac{d\psi_{sd}}{dt} - \omega_e \psi_{sq} + R_s i_{sd} \\ u_{sq} = \dfrac{d\psi_{sq}}{dt} + \omega_e \psi_{sd} + R_s i_{sq} \end{cases} \tag{5}$$

$$\begin{cases} u_{rd} = \dfrac{d\psi_{rd}}{dt} - s\omega_e \psi_{rq} + R_r i_{rd} \\ u_{rq} = \dfrac{d\psi_{rq}}{dt} + s\omega_e \psi_{rd} + R_r i_{rq} \end{cases} \tag{6}$$

Where, R is the resistance, L is the inductance, U is the voltage; I is the current, ψ is the flux, subscript m is the mutual interaction component, subscript s is the stator component, subscript r is the rotor component.

The stator and rotor flux plural vector model of DFIG can be expressed by (7) and (8) respectively in the *dq* rotating reference frame [4].

$$\begin{cases} \psi_{sd} = L_s i_{sd} + L_m i_{rd} \\ \psi_{sq} = L_s i_{sq} + L_m i_{rq} \end{cases} \tag{7}$$

$$\begin{cases} \psi_{rd} = L_r i_{rd} + L_m i_{sd} \\ \psi_{rq} = L_r i_{rq} + L_m i_{sq} \end{cases} \tag{8}$$

The maximum power point tracking (MPPT) control is completed through controlling rotor speed. The reactive power voltage control of DFIG is provided by controlling the rotor excitation voltage amplitude and phase angle. The output active power and reactive power of DFIG can be independently controlled according to feed-forward compensation method. Making the d axis of synchronously rotating reference frame coincide with stator voltage vector, where $u_{sd}=U_S$, $u_{sq}=0$. Ignoring the stator electromagnetic transient process and the stator resistance voltage dip of DFIG, the rotor voltage control equation is expressed as (9) according to (5)-(8).

$$\begin{cases} u_{rd} = R_r i_{rd} + \sigma L_r \dfrac{d}{dt} i_{rd} - s\omega_e \sigma L_r i_{rq} + s \dfrac{L_m}{L_s} U_S \\ u_{rq} = R_r i_{rq} + \sigma L_r \dfrac{d}{dt} i_{rq} + s\omega_e \sigma L_r i_{rd} \end{cases} \tag{9}$$

Where, $\sigma=1-L_m^2/(L_sL_r)$.

The rotor active and reactive current components are completely decoupling, but the corresponding control voltage vector is not completely decoupling. The voltage decoupling control can be implemented by additional feed-forward input $-s\omega_e \sigma L_r i_{rq} + s\dfrac{L_m}{L_s}U_S$ and $s\omega_e \sigma L_r i_{rd}$ respectively.

Assuming that a three-phase short circuit fault occurs in a radial system, the voltage sag conditions can be formulated using the voltage-divider model according to (5) and (6). The equivalent circuit of power system connection of DFIG is shown in Fig. 2 [4].

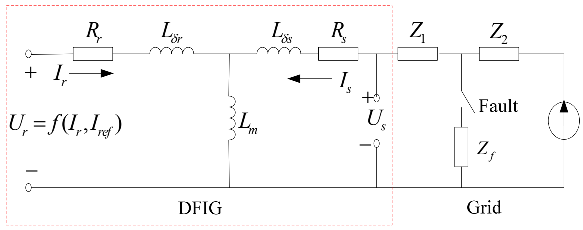

Fig. 2 The equivalent circuit of power system

In Fig. 2, the voltage and current relation of power grid is given as follows in the steady-state condition.

$$U_0 = U_{s0} + Z_0 I_{s0} \tag{10}$$

Where, U_0 is the grid voltage, U_{s0} is the terminal steady-state voltage, I_{s0} is the stator steady-state current, $Z_0=Z_1+Z_2$ is the transmission line impedance.

Ignoring the transient process of converter switch, assuming the rotor current is equal to its reference value. The voltage, current and flux vector of DFIG can be considered stationary, and the generator flux is constant. The terminal voltage can be calculated through grid voltage and rotor current according to (5), (6) and (10) as follows.

$$U_{s0} = \frac{Z_s}{Z_0 + Z_s} U_0 + \frac{jX_m Z_0}{Z_0 + Z_s} I_{r0} \tag{11}$$

Where, $Z_s=R_s+j\omega_e L_s$, $X_m=\omega_e L_m$, I_{r0} is the rotor steady-state current.

As shown in Fig. 2, when a grid fault occurs, the structure of power grid changes immediately, and the control mode of DFIG will switch. Then the voltage and current relation of power grid can be given by (12).

$$U_0 = (1 + \frac{Z_2}{Z_f})U_{sf} + (Z_0 + \frac{Z_1 Z_2}{Z_f})I_{sf} \tag{12}$$

Where, U_{sf} is the terminal fault voltage, I_{sf} is the stator fault current, Z_f is the grounding resistance.

Ignoring the transient process of stator and rotor, the terminal fault voltage can be calculated through grid voltage and rotor fault current according to (5), (6) and (12) as follows.

$$\begin{aligned} U_{sf} &= \frac{Z_f Z_s}{Z_f Z_s + Z_2 Z_s + Z_f Z_0 + Z_1 Z_2} U_0 \\ &+ \frac{jX_m (Z_0 Z_f + Z_1 Z_2)}{Z_f Z_s + Z_2 Z_s + Z_f Z_0 + Z_1 Z_2} I_{rf} \end{aligned} \tag{13}$$

Where, I_{rf} is the rotor fault current.

When a short circuit fault occurs, the voltage magnitude drop, and the voltage phase angle of power grid with large-scale DFIG integration also jumps. According to (5), (6), (11) and (13), the terminal voltage change value can be given by (14).

$$\begin{aligned} \Delta U_s &= U_{sf} - U_{s0} \\ &= (\frac{Z_f Z_s}{Z_f Z_s + Z_2 Z_s + Z_f Z_0 + Z_1 Z_2} - \frac{Z_s}{Z_0 + Z_s})U_0 \\ &+ \frac{jX_m (Z_0 Z_f + Z_1 Z_2)}{Z_f Z_s + Z_2 Z_s + Z_f Z_0 + Z_1 Z_2} I_{rf} - \frac{jX_m Z_0}{Z_0 + Z_s} I_{r0} \end{aligned} \tag{14}$$

The voltage phase angle jump value can be calculated by (15) when a grid fault occurs.

$$\Delta\varphi = \arctan(\Delta U_s) \tag{15}$$

The voltage phase angle jump value is nearby after the grid fault and the grid fault occurs, which can be calculated by (16).

$$\Delta\varphi' \approx -\Delta\varphi \tag{16}$$

The rotor steady-state current I_{r0} and the rotor fault current I_{rf} can be given by the control strategy of DFIG.

III. ANALYSIS OF OPERATION CHARACTERISTICS OF DFIG UNDER VOLTAGE PHASE ANGLE JUMP

The voltage phase angle jump influences phase angle tracking accuracy of DFIG, and the *dq* axis decoupling control conditions based on stator voltage orientation method are destroyed. This section is aimed to reveal the response characteristics of PLL, evaluate the effectiveness of traditional control strategy of DFIG.

A. Response characteristics of PLL

For ensuring the grid synchronization of power electronic converters, phase-Locked Loop (PLL) is widely used. PLL is a closed-loop dynamic system, generally speaking, PLL consists of phase detector (PD), loop filter (LF), and voltage controlled oscillator (VCO). The structure of a typical PLL of DFIG is shown in Fig. 3.

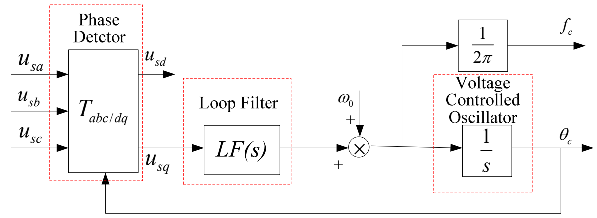

Fig. 3 The structure of a typical PLL of DFIG

The loop filter $LF(s)$ is a proportional plus integral controller, and $LF(s)=k_p+k_i/s$, k_p is the proportional gain, k_i is the integral gain. The parameters k_p and k_i need to meet the closed-loop performance specifications. The VCO function is an integrator. According to Fig. 3, the open-loop transfer function of PLL are as follows.

$$G(s) = \frac{2\zeta\omega_c s + \omega_c^2}{s^2 + 2\zeta\omega_c s + \omega_c^2} \tag{17}$$

Where, ω_c is the natural frequency, ζ is the damping factor, which can be given by (18).

$$\begin{cases} \omega_c = \sqrt{k_i} \\ \zeta = \dfrac{k_p}{2\sqrt{k_i}} \end{cases} \tag{18}$$

We know that the values of ω_c and ζ determine the parameters of PLL, i.e. k_p and k_i from (18). Furthermore, the allowable variation ranges of ω_c and ζ are given based on the stability requirements of power grid and actual demand. According to the above analysis, there is a voltage phase angle jump $\Delta\varphi$ under a serious grid fault when large-scale DFIG are connected into power grid. The transfer function of phase angle error can be expressed by (19) in Fig. 3.

$$\theta_c^{\Delta\varphi}(s) = \frac{\Delta\varphi}{s} G(s) = \frac{2\zeta\omega_c s + \omega_c^2}{s(s^2 + 2\zeta\omega_c s + \omega_c^2)} \Delta\varphi \tag{19}$$

The step response tracking errors $\Delta\theta_c^{\Delta\varphi}(t)$ of phase angle jump in time domain can be given by (20) by Laplace inverse transformation based on (19) [31].

$$\Delta\theta_c^{\Delta\varphi}(t) = \begin{cases} \left\{ e^{-\zeta\omega_c t}[\cos(\omega_c t\sqrt{1-\zeta^2}) + \dfrac{\zeta\sqrt{1-\zeta^2}}{1-\zeta^2}\sin(\omega_c t\sqrt{1-\zeta^2})] \right\} \Delta\varphi & 0 < \zeta < 1 \\ (e^{-\omega_c t} - \omega_c t e^{-\omega_c t})\Delta\varphi & \zeta = 1 \\ [\dfrac{1}{2}(1 - \dfrac{\zeta\sqrt{\zeta^2-1}}{\zeta^2-1}) e^{-(\zeta-\sqrt{\zeta^2-1})\omega_c t} + \dfrac{1}{2}(1 + \dfrac{\zeta\sqrt{\zeta^2-1}}{\zeta^2-1}) e^{-(\zeta+\sqrt{\zeta^2-1})\omega_c t}]\Delta\varphi & \zeta > 1 \end{cases} \tag{20}$$

According to (20), Fig. 4 shows the tracking errors of PLL in the condition of different control parameters of PLL.

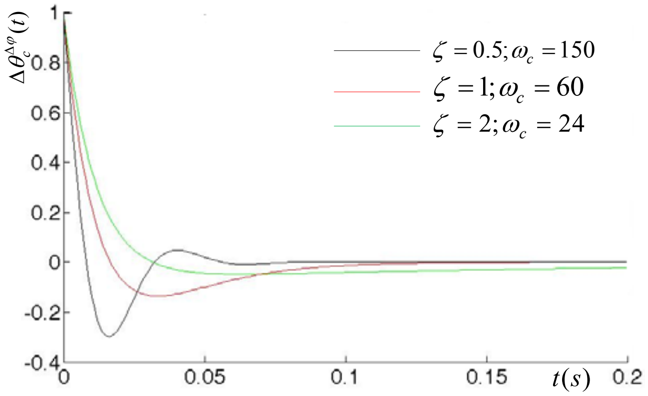

Fig. 4 Tracking errors of PLL to voltage phase angle jump

Fig. 4 and (20) show the phase angle deviation $\Delta\theta$ and its dynamic characteristics between actual and measured *dq* rotating reference frame. The phase angle deviation is restricted by PLL technology. The higher natural frequency ω_c, the smaller damping factor ζ, and the faster transient response, the bigger overshoot. A larger value of ω_c decreases the disturbance rejection capability of PLL, and the damping factor ζ has relatively less effect.

B. Impacts of voltage phase angle jump on the control characteristic of DFIG

The phase angle deviation $\Delta\theta$ as shown in Fig.4 will influence the decoupling control of DFIG based on stator voltage orientation method. The *d* axis orientation voltage and *q* axis orientation voltage will change, i.e., $u_{sd1}=U_s\cdot\cos\Delta\theta$, $u_{sq1}=U_s\cdot\sin\Delta\theta$. According to the designed method of RSC control strategy based on stator voltage orientation method, the voltage vector model of DFIG can be expressed by (21) based on (5).

$$\begin{cases} u_{sd1} = -\omega_e \psi_{sq} = U_S \cos\Delta\theta \\ u_{sq1} = \omega_e \psi_{sd} = U_S \sin\Delta\theta \end{cases} \tag{21}$$

Then the flux plural vector model of DFIG can be expressed by (22) based on (7) and (21).

$$\begin{cases} \psi_{sd1} = L_s i_{sd} + L_m i_{rd} = \dfrac{U_S \sin\Delta\theta}{\omega_e} \\ \psi_{sq1} = L_s i_{sq} + L_m i_{rq} = -\dfrac{U_S \cos\Delta\theta}{\omega_e} \end{cases} \tag{22}$$

The stator current can be expressed as (23).

$$\begin{cases} i_{sd} = \dfrac{U_s \sin\Delta\theta}{\omega_e L_s} - \dfrac{L_m}{L_s} i_{rd} \\ i_{sq} = -\dfrac{U_s \cos\Delta\theta}{\omega_e L_s} - \dfrac{L_m}{L_s} i_{rq} \end{cases} \tag{23}$$

Not considering the stator electromagnetic transient process and the stator resistance voltage dip of DFIG. According to (5)–(8) and (23), the rotor voltage control equation is expressed as (24).

$$\begin{cases} u_{rd1} = R_r i_{rd} + \sigma L_r \dfrac{di_{rd}}{dt} - s\omega_e \sigma L_r i_{rq} + s\dfrac{L_m}{L_s} U_s \cos\Delta\theta \\ u_{rq1} = R_r i_{rq} + \sigma L_r \dfrac{di_{rq}}{dt} + s\omega_e \sigma L_r i_{rd} + s\dfrac{L_m}{L_s} U_s \sin\Delta\theta \end{cases} \tag{24}$$

Where, the rotor active and reactive current components are completely decoupling, but the corresponding control voltage vector is not decoupling. The rotor *d* axis voltage vector and the rotor *q* axis voltage vector are functions of rotor *d* axis current, rotor *q* axis current and phase angle deviation, respectively. Therefore, the voltage decoupling control can't be implemented only by additional feed-forward input $-s\omega_e \sigma L_r i_{rq} + s\dfrac{L_m}{L_s} U_S$ and $s\omega_e \sigma L_r i_{rd}$ respectively.

IV. FRT STRATEGY OF DFIG USING ROTOR VOLTAGE DIRECT COMPENSATION CONTROL BASED ON VOLTAGE PHASE ANGLE DEVIATION

We know that there is a voltage phase angle jump of DFIG if there is a serious grid fault. The jump value is affected by FRT strategy of DFIG. In addition, the phase angle deviation between actual and measured *dq* rotating reference frame is restricted by PLL technology. The phase angle deviation broken the active power and reactive power decoupling control of DFIG, weaken the FRT capability, and may cause FRT failure of DFIG. For improving the controllability and stability of DFIG, a FRT strategy of DFIG using rotor voltage direct compensation control based on voltage phase angle deviation is proposed in the paper.

The relation of rotor voltage control equation can be expressed as follows based on (9) and (24) considering voltage phase angle jump.

$$\begin{cases} u_{rd1} = u_{rd} + \Delta u_{rd}(\Delta\theta) \\ u_{rq1} = u_{rq} + \Delta u_{rq}(\Delta\theta) \end{cases} \tag{25}$$

Where, u_{rd1} is the rotor *d* axis control voltage, u_{rq1} is the rotor *q* axis control voltage under voltage phase angle jump. $\Delta u_{rd}(\Delta\theta)$ is the rotor *d* axis control voltage compensation component, $\Delta u_{rq}(\Delta\theta)$ is the rotor *q* axis control voltage compensation component, which are given by (26).

$$\begin{cases} \Delta u_{rd}(\Delta\theta) = s\dfrac{L_m}{L_s} U_s (\cos\Delta\theta - 1) \\ \Delta u_{rq}(\Delta\theta) = s\dfrac{L_m}{L_s} U_s \sin\Delta\theta \end{cases} \tag{26}$$

According to (25) and (26), the basic principle of FRT strategy of DFIG using rotor voltage direct compensation control based on voltage phase angle deviation is presented in Fig.5. The proposed FRT strategy increases a compensation component in traditional FRT control structure for ensuring control accuracy and FRT capability of DFIG.

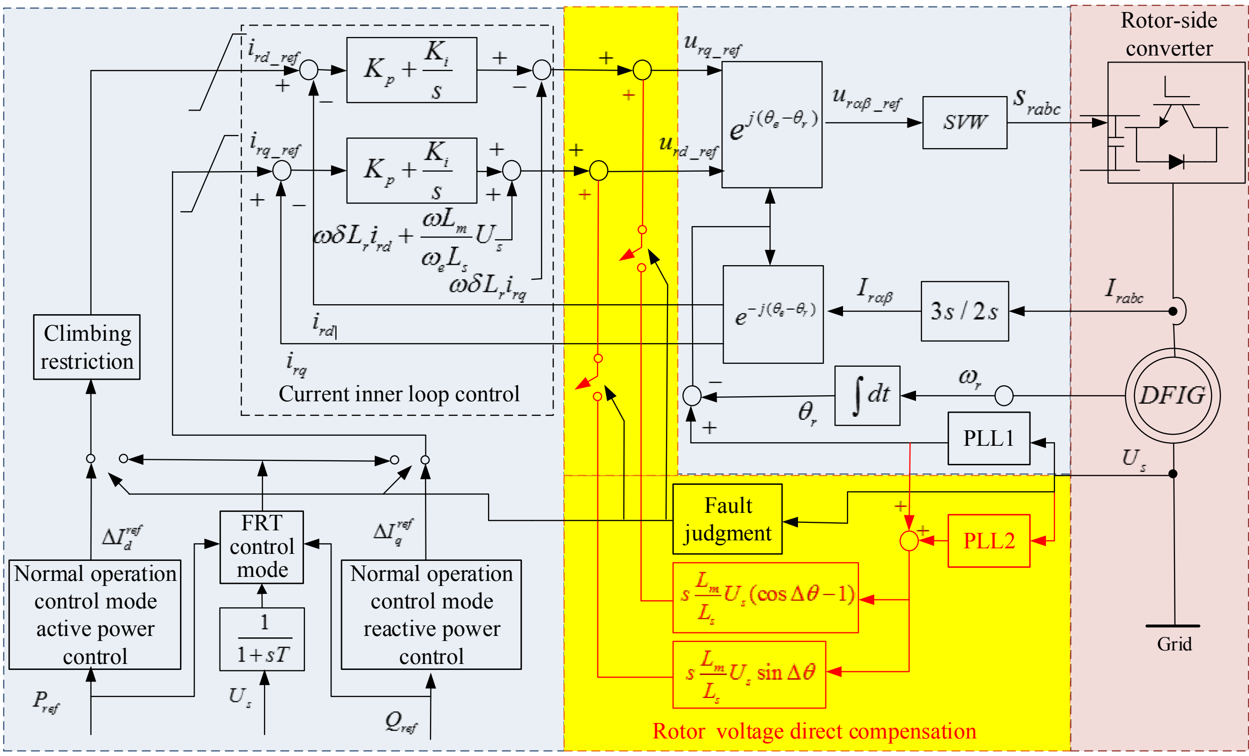

Fig. 5 FRT strategy of DFIG using rotor voltage direct compensation control based on voltage phase angle deviation

The proposed control strategy of DFIG in Fig.5 includes two operation control modes. Mode 1: normal operation control mode, the active power and reactive power decoupling control are implemented using traditional single PLL when the voltage phase angle is constant. Mode 2: FRT operation control mode, where the double PLLs are implemented. On the one hand, the slower response speed of PLL1 is adopted for increasing the system damping, and the rotating reference frame is given by which. On the other hand, the faster response speed of PLL2 is adopted for guaranteeing the control accuracy and capability of DFIG. The structure of PLL1 and PLL2 are shown in Fig 3. At the same time, the rotor voltage compensation component is increased in FRT strategy based on (25) and (26), the phase angle deviation is obtained by PLL1 and PLL2. The stability and control capability of DFIG are simultaneously improved.

The detailed flow of FRT strategy of DFIG using rotor voltage direct compensation control based on voltage phase angle deviation is described as follows.

Step 1: Obtain the measured terminal voltage signal U_s.

Step 2: Make a judgment on the terminal voltage U_s. When the terminal voltage U_s is less than 0.9pu, DFIG will transfer to FRT operation control mode, and the rotor voltage direct compensation module is activated.

Step 3: If the terminal voltage U_s is first up to 0.9pu, the period between 0s~10s after which is defined as post-fault period. The FRT operation control mode is still activated, and the rotor voltage direct compensation module is also activated.

Step 4: The period is steady state period when the terminal voltage U_s is up to 0.9pu after10s, DFIG will transfer to normal operation control mode.

V. SIMULATION ANALYSIS

For verifying the accuracy and effectiveness of proposed FRT strategy of DFIG using rotor voltage direct compensation control based on voltage phase angle deviation in the paper, an actual power grid with large-scale DFIG is provided in the section. Fig. 6 shows the structure of study system, the installed capacity of wind farm 1 is 250MW, an aggregated model of which based on multiply equivalent method is adopted in appendix A1. Wind farm 1 is chosen as the study target for this case, equipped with 2MW DFIG based wind turbines. The parameters are obtained from an actual operation of DFIG, i.e., U_N=690V, R_s=0.01pu, R_r=0.01pu, L_s=0.1pu, L_r=0.1pu, L_m=3.5pu. Wind farm 1 is connected into 220kV Substation 1 via 100km AC transmission line, the resistance of which is 0.04Ω/km, the inductance is 0.41mH/km. The damping factor ζ=0.707, the reference natural frequency ω_{cN}=120 in PLL1. The damping factor ζ=0.35, the reference natural frequency ω_{cN}=300 in PLL2. Supposing that the crowbar protection of DFIG is inactivated, and the DFIG is controlled during the grid fault.

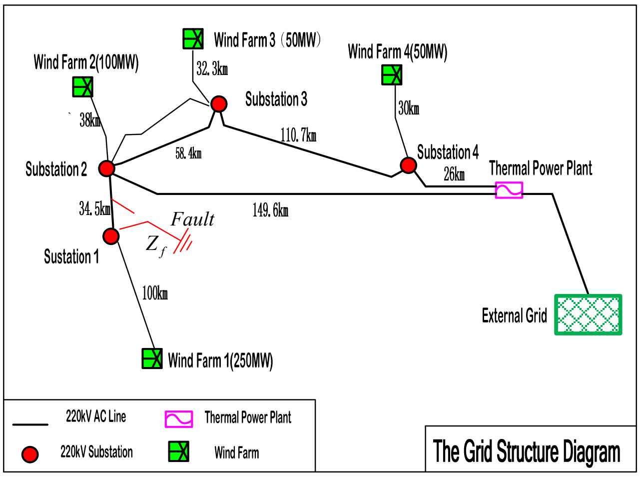

Fig. 6 Structure of study system

Assuming that there is a short circuit fault as shown in Fig.6, and the grid fault is cleared after 120 milliseconds. The simulations are designed to analyze the accuracy and effectiveness of proposed FRT strategy of DFIG in different output active power conditions.

A. Analysis of transient characteristics of DFIG under high output active power

The transient characteristics of DFIG are shown in Fig.7 under high output active power. As shown in Fig. 7, when a grid fault occurs and the traditional FRT strategy of DFIG is adopted under high output active power, the minimum voltage amplitude drop value is 0.202pu; the maximum voltage phase angle jump value is 57.68°; the output efficacious reactive power of wind farm 1 is 35.8Mvar. While the minimum voltage amplitude drop value is 0.237pu when the proposed FRT strategy of DFIG is adopted; the maximum voltage phase angle jump value is 29.14°; the output efficacious reactive power of wind farm 1 is 46.4Mvar. So the output power of wind farm can be guaranteed using the proposed FRT strategy of DFIG under high output active power during the grid fault, and the voltage stability of system is stronger.

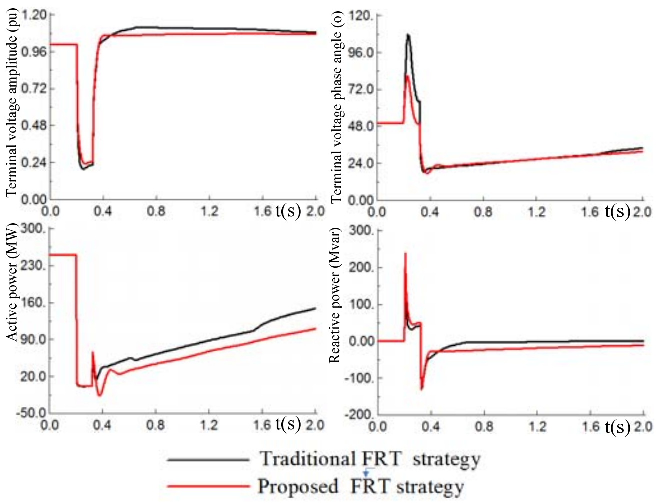

Fig. 7 Transient characteristics of DFIG under high output active power

B. Analysis of transient characteristics of DFIG under low output active power

The transient characteristics of DFIG are shown in Fig.8 under low output active power. As shown in Fig. 8, when a grid fault occurs and the traditional FRT strategy of DFIG is adopted under low output active power, the minimum voltage amplitude drop value is 0.201pu; the maximum voltage phase angle jump value is 32.61°; the output efficacious reactive power of wind farm 1 is 35.8Mvar. While the minimum voltage amplitude drop value is 0.239pu when the proposed FRT strategy of DFIG is adopted; the maximum voltage phase angle jump value is 15.14°; the output efficacious reactive power of wind farm 1 is 44.35Mvar. So the output power of wind farm can also be guaranteed using the proposed FRT strategy of DFIG under low output active power during the grid fault, and the voltage stability of system is stronger.

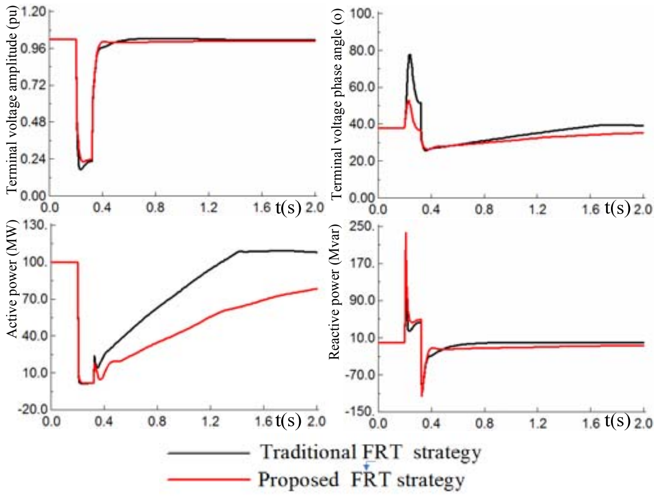

Fig. 8 Transient characteristics of DFIG under low output active power

Therefore, the advantages of proposed FRT strategy of DFIG using rotor voltage direct compensation control based on voltage phase angle deviation can be summarized as follows. 1) The accuracy of output active power and reactive power of DFIG can be guaranteed, 2) The transient characteristics of power grid with large-scale DFIG integration can be optimized under voltage phase angle jump.

VI. CONCLUSION

This paper has revealed the physical mechanism of DFIG under voltage phase angle jump. Then, the operation characteristics of DFIG are analyzed. Meanwhile, based on the voltage phase angle deviation this paper has developed a FRT strategy of DFIG using rotor voltage direct compensation control. For clear illustrations, the following conclusions can be highlighted.

1) The internal voltage phase angle of DFIG is not related to rotor position, and the voltage phase angle jumps when a grid fault occurs.

2) The voltage phase angle jump destroy *dq* axis decoupling performance of DFIG based on stator voltage orientated method, thereby result in decreasing the FRT capability of

DFIG.

3) The proposed FRT strategy of DFIG adds a compensation component to the commanded rotor voltage based on the voltage phase angle deviation. By this means, the decoupling control of DFIG can be achieved with the higher accuracy.

4) The proposed FRT strategy optimizes the transient characteristics of DFIG. Then, the FRT capability of power grid with large-scale DFIG integration is also improved.

APPENDIX

A1 Structure diagram of wind farm 1

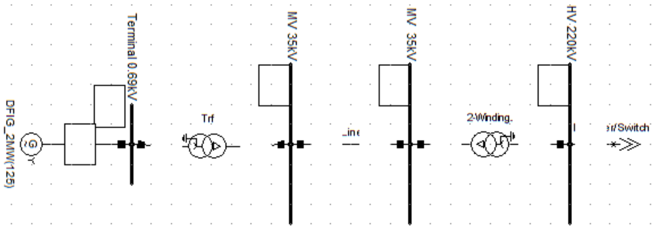

REFERENCES

[1] China installed wind power capacity. Chinese wind energy association (2015), Beijing China, 2016.

[2] Y.N. Chi, “Studies on the stability issues about large scale wind farm grid integration.” China Electric Power Research Institute, 2006.

[3] Y.K. He, J.B. Hu, “Several hot-spot issues associated with the grid-connected operations of wind-turbine driven doubly fed induction generators.” PCSEE, vol. 32, no. 27, pp: 1-15, 2012.

[4] X.S. Tian, G.Y. Li, Y.N. Chi, et al, “Voltage phase angle jump characteristic of DFIGs in case of weak grid connection and grid fault.” J. Mod. Power Syst. Clean Energy, vol. 4, no. 2, pp: 256-264, 2016.

[5] Goksu O, Teodorescu R, Bak CL et al, “Instability of wind turbine converters during current injection to low voltage grid faults and PLL frequency based stability solution.” IEEE Trans Power Syst, vol. 29, no. 4, pp: 1683-1691, 2014.

[6] W.J. Chen, D.H. Xu, N. Zhu, M. Chen, and Frede Blaabjerg, et al, “Control of doubly-fed induction generator to ride-through recurring grid faults.” IEEE TRANSACTIONS ON POWER ELECTRONICS, vol. 31, no. 7, pp: 4831-4846, 2016.

[7] S. Abulanwar; Energy Technol. Dept., Aalborg Univ. et al, “Improved FRT control scheme for DFIG wind turbine connected to a weak grid.” In: 2013 IEEE PES Asia-Pacific Power and Energy Engineering Conference (APPEEC), Kowloon, Dec, 2013, pp: 1-6.

[8] X.G. Liu, Z. Xu, Kit Po WONG, “Recent advancement on technical requirements for grid integration of wind power.” J. Mod. Power Syst. Clean Energy, vol. 1, no. 3, pp: 16-22, 2013.

[9] Morren J, de Haan SWH, “Short-circuit current of wind turbines with doubly fed induction generator.” IEEE Trans Energy Convers, vol. 22, no. 1, pp: 174-180, 2007.

[10] X.P. Kong, Z. Zhang, X.G. Yin, et al, “Study of fault current characteristics of DFIG considering impact of crowbar protection.” Trans of China Electrotechnical Society, vol. 30, no. 8, pp: 1-10, 2015.

[11] Gabriela Nicoleta Sava; Minh Quan Duong; Sonia Leva, et al, “Coordination control of active crowbar for doubly fed induction generators.” In: 2014 International Symposium on Fundamentals of Electrical Engineering (ISFEE), Bucharest, Nov, 2014, pp: 1-5.

[12] Rahimi M, Parniani M, “Grid-fault ride-through analysis and control of wind turbines with doubly fed induction generators.” Electr Power Syst Res, vol. 80, no. 2, pp: 184-195, 2010.

[13] Lopez J, Sanchis P, Roboa X, “Dynamic behavior of the doubly fed induction generator during three-phase voltage dips.” IEEE Trans Energy Convers, vol. 22, no. 3, pp: 709-717, 2007.

[14] Jackson John Justo, Francis Mwasilu, and Jin-Woo Jung, “Doubly fed induction generator wind turbines: A novel integrated protection circuit for low-voltage ride-through strategy.” JOURNAL OF RENEWABLE AND SUSTAINABLE ENERGY, vol. 6, no. 5, pp: 1-15, 2014.

[15] X.S. Tian, W.S. Wang, Y.N. Chi, et al, “Performances of DFIG-based wind turbines during system fault and its impact on transient stability of power system.” Automat Electr Power Syst, vol. 39, no. 10, pp: 16-21, 2015.

[16] Vittal E, O’Malley M, Keane A, “Rotor angle stability with high penetrations of wind generation.” IEEE Transactions on Power System, vol. 27, no. 1, pp: 353-362, 2012.

[17] J. Ma, X.B. Lan, X.X. Ding, et al, “Transient Characteristics of Symmetrical Short Circuit Fault in Double Fed Induction Generators Considering Grid-Side Converter Control and Phase-Angle Jump of DFIG’s Terminal Voltage” Power System Technology, vol. 38, no. 7, pp: 1891-1897, 2014.

[18] Elisa Espinosa Juairez, Araceli Hernaindez, “Stochastic assessment of phase-angle jumps caused by voltage sags applying an analytical method.” 9th International Conference on Probabilistic Methods Applied to Power Systems, KTH, Stockholm, Sweden, June, 2006. pp: 1-6.

[19] Mansour M, Islam S, Masoum MAS, “Impacts of symmetrical and asymmetrical voltage sags on DFIG-based wind turbines considering phase-angle jump, voltage recovery, and sag parameters.” IEEE Trans. Power Electron, vol. 26, no. 5, pp: 1587-1598, 2011.

[20] Y. Zhang, Z.C. Zou, Y. Lin, D.S. Hhuang, X.Y. Xiao, F. Lin, “Rotor voltage dynamic characteristics of doubly-fed induction generator with phase angle jump.” Automation of electric power systems. vol. 40, no. 17, pp: 129-136, 2016.

[21] X.F. Xiong, J.X. Ouyang, A. Wen, “An analysis on impacts and characteristics of voltage of DFIG-based wind turbine generator under grid short circuit.” Automation of Electric Power Systems vol. 36, no. 14, pp: 143-149, 2012.

[22] Y. Wang, Q.W. Wu, “Electromagnetic transient response analysis of DFIG under cascading grid faults considering phase angel jumps.” In: 17th International Conference on Electrical Machines and Systems (ICEMS 2014), Hangzhou, China, Oct 2014, PP: 1340-1344.

[23] Y. Zhang, Z.C. Zhou, Y. Lin, et al, “Rotor Voltage Dynamic Characteristics of Doubly-fed Induction Generator with Phase Angle Jump.” Automation of Electric Power Systems vol. 40, no. 17, pp: 129-136, 2016.

[24] H.L. Xu, W. Zhang, J.B. Hu, et al, “Synchronizing signal detection of fundamental voltage under unbalanced and/or distorted grid voltage condition.” Automation of Electric Power Systems, vol. 36, no. 5, pp: 90-95, 2012.

[25] X. Du, G.N. Wang, P.J. Sun, et al, “Synchronization signal detection for grid fundamental voltage through employing sinusoidal amplitude integrators.” PCSEE, vol. 33, no. 36, pp: 104-111, 2013.

[26] X.P. Pei, X.H. Hao, W. Chen, “A novel three-phase phase-locked-loop system based on model reference adaptive algorithm.” Trans of China Electrotechnical Society, vol. 29, no. 4, pp: 196-204, 2014.

[27] Y. Wang, Math H. J. Bollen, and X.Y. Xiao, “Calculation of the phase-angle-jump for voltage dips in three-phase systems.” IEEE TRANSACTIONS ON POWER DELIVERY, vol. 30, no. 1, pp: 480-487, 2015.

[28] D.L. Zhang, Y.J. Wang, J.B. Hu, S.C. Ma, Q. He, and Q. Guo, “Impacts of PLL on the DFIG-based WTG’s electromechanical response under transient conditions: analysis and modeling.” CSEE JOURNAL OF POWER AND ENERGY SYSTEMS, vol. 2, no. 2, pp: 30-39, 2016.

[29] W. Wang, N. Chen, N.C. Zhu, et al, “Phase angle compensation control strategy for low-voltage ride through of doubly-fed induction generator.” PCSEE, vol. 29, no. 21, pp: 62-68, 2009.

[30] Y.X. Ni, S.S Chen, B.L. Zhang, “Theory and analysis of dynamics power system,” Beijing, China, Tsinghua university press, 2002.

[31] S.S Hu., “Automatic control theory.” Beijing, China, National Defence Industrial Press, 2000.

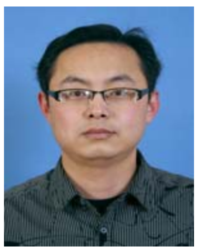

Xinshou Tian was born in 1985. He received his B.E. degree from Huazhong University of Science and Technology, China, in 2008, M.E. degree from China Electric Power Research Institute, China, in 2011, and Ph.D. degree in electrical engineering from North China Electricity Power University, China, in 2016. Since 2016 he has been employed at China Electric Power Research Institute (CEPRI), Beijing, China. His main research interests include wind power generation and power system stability analysis.

Weisheng Wang received his B.E. and M.E. degrees from Xi'an University of Technology, China, in 1990, and 1993, respectively, and Ph.D. degree in electrical engineering from Xi'an Jiaotong University, China, in 1996. Since 1997 he has been employed at China Electric Power Research Institute (CEPRI), Beijing, China, where he is the senior engineer (professor) and director of Renewable Energy Department of CEPRI. His research of interests is in integration of renewable energy generation.

Xiang Li was born in 1990. She received her B.E. degree in Tsinghua University, China, in 2008, and M.E. degree from China Electric Power Research Institute, China in 2016. Since 2016 she has been employed at State Grid Beijing Changping Electric Power Supply Company, China. Her main research interests include wind power integration and power system stability analysis.

Yongning Chi received his B.E. and M.E. degrees from Shandong University, China, in 1995, and 2002, respectively, and Ph.D. degree in electrical engineering from China Electric Power Research Institute, China, in 2006. Since 2003 he has been employed at China Electric Power Research Institute (CEPRI), Beijing, China, where he is the chief engineer for Renewable Energy Department. His research of interests is in modeling, control and integration analysis of renewable energy generation.

Yan Li received his B.S. degree from Shandong University of Technology in 1999, and received his M.S. degree from Fuzhou University in 2002, and received his Ph.D. degree from China Electric Power Research Institute (CEPRI) in 2007. Since 2007 he has been employed at CEPRI, presently as Renewable Energy Integration Planning and Simulation Research Division director of Renewable Energy Department of CEPRI. His interested researches are the power system analysis, renewable energy modeling and grid integration simulation, renewable energy develop planning.

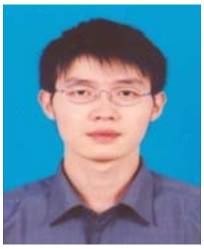

Haiyan Tang received his B.E. and M.E. degrees from Hefei University of Technology, China, in 2000, and 2003, respectively, and Ph.D. degree in electrical engineering from China Electric Power Research Institute, China, in 2008. Since 2008 he has been employed at China Electric Power Research Institute (CEPRI), Beijing, China. His research of interests is in modeling, control and integration analysis of renewable energy generation.